Korean J. Chem. Eng., 34(4), 1062-1072 (2017)
DOI: 10.1007/s11814-016-0343-8

pISSN: 0256-1115
eISSN: 1975-7220

Comparative study of electrocoagulation and electrochemical Fenton treatment of aqueous solution of benzoic acid (BA): Optimization of process and sludge analysis

Vishal Kumar Sandhwar† and Basheshwer Prasad

Department of Chemical Engineering, Indian Institute of Technology Roorkee, Roorkee-247667 (Uttarakhand), India
(*Received 19 August 2016 • accepted 29 November 2016*)

Abstract−Benzoic acid containing synthetic solution was pretreated by acid precipitation at various pH (1-3) and temperature (15-60 °C). Pre-treated solution was further treated by electrocoagulation (EC) and electrochemical Fenton (EF) processes using iron anode and graphite cathode. Optimization of independent operating parameters, namely, initial pH: (3-11), current density (A/m^2): (15.24-76.21), electrolyte concentration (mol/L): (0.03-0.07) and electrolysis time (min): (15-95) for EC process and pH: (1-5), current density (A/m^2): (15.24-76.21), H_2O_2 concentration (mg/L): (100-500) and electrolysis time (min): (15-95) for EF process, was performed using central composite design (CCD) in response surface methodology (RSM). Maximum removal efficiencies of BA- 76.83%, 88.50%; chemical oxygen demand (COD) - 69.23%, 82.21% and energy consumption (kWh/kg COD removed) - 30.86, 21.15 were achieved by EC and EF processes, respectively, at optimum operating conditions. It was found that EF process is more efficient than EC process based on removal of BA and COD with lower energy consumption. The sludge obtained after EC and EF treatments was analyzed by XRD, FTIR, DTA/TGA and SEM/EDX techniques.

Keywords: Benzoic Acid, Electrocoagulation, Electrochemical Fenton, Optimization, Sludge Analysis

INTRODUCTION

Petrochemical wastewater consists of toxic compounds in very high concentration which emanate during production of petrochemicals such as olefins and aromatics. Purified terephthalic acid (PTA) is an xylene-based aromatic compound manufactured by air oxidation of para-xylene in the presence of cobalt or manganese salt catalyst with bromine promoter [1]. PTA is widely used as raw material for the manufacture of plastic bottles, pesticides, textile fibers, dyes and polyester films [1,2]. During PTA production, large numbers of pollutants are emitted in environment and a major part is released in the water environment. The wastewater generally emerges from the catalyst recovery unit, scrubbing unit, cleaning and washing section of PTA plant [3]. Approximately 3-4 m^3 wastewater with 5-20 g/L of chemical oxygen demand (COD) is generated per ton of PTA production [4]. PTA wastewater contains several major aromatic compounds like para-toluic acid (p-TA), benzoic acid (BA), phthalic acid (PA), terephthalic acid (TA), acetic acid (AA), 4-carboxybenzaldehyde with minor concentration of some aromatic compounds like 4-formylbenzoic acid, p-xylene and methyl acetate [5-9]. Due to the high toxicity of p-TA, TPA and BA, the United States Environmental Protection Agency (USEPA) has included these aromatics in the list of priority pollutants [10-12]. They are known to cause both acute and chronic toxicity, molecular toxicity and are also responsible for the damage of bladder, kidneys, liver and histopathological abnormalities [13-16]. World Health Organization suggested that the maximum intake limit of benzoic acid for human being should be less than 5 mg/kg of body weight per day [17-19]. Central Pollution Control Board (CPCB) of India has prescribed a discharge limit of COD less than 250 mg/L into surface waters for petrochemical industry [20]. Therefore, to achieve the required discharge quality standards, the PTA wastewater has to be extensively treated before being allowed to discharge into surface water bodies. Various phisico-chemical treatment technologies have been used in past for the treatment of petrochemical wastewater. However, due to automation, high efficiency and low sludge generation features, electrochemical methods like electrocoagulation and electrochemical Fenton are now being effectively used for wastewater remediation [21-23].

1. Electrocoagulation (EC)

In EC, coagulants are generated in situ by electrically dissolving metal ions from metal electrodes. Metal ion generation occurs at the anode surface, while hydrogen gas is produced at the cathode. Flocs of metal hydroxides formed during coagulation, remove the organics from the solution through charge neutralization, adsorption and sweep flocculation. Eventually these flocs are separated from the solution through sedimentation or flotation [24,25]. Following reactions represent the EC process:

At cathode:

$$2H_2O+2e^- \rightarrow H_2+2OH^- \quad (1)$$

At anode:

$$2Fe_{(s)} \rightarrow 2Fe^{2+}_{(aq)}+4e^- \quad (2)$$

$$Fe^{2+}_{(aq)}+2OH^-_{(aq)} \rightarrow Fe(OH)_{2(s)} \quad (3)$$

In the solution:

$$Fe^{+3}_{(aq)}+H_2O \rightarrow Fe(OH)^{2+}_{(aq)}+2H^+_{(aq)} \quad (4)$$

2. Electrochemical Fenton (EF)

Electrochemical Fenton is a type of electro-Fenton process. Elec-

†To whom correspondence should be addressed.
E-mail: vksandhwar@gmail.com

tro-Fenton is an eco-friendly and one of the most popular electrochemical advance oxidation processes based on Fenton's reaction chemistry [26,27]. Electro-Fenton process has two distinct configurations. First, is the addition of the Fenton reagents from outside to the reactor having inert electrode. In second, only hydrogen peroxide (H_2O_2) is added from outside to the reactor and Fe^{2+} ions are generated through sacrificial iron anode [28]. The following chain reactions explain the degradation of organic pollutants by Fenton process [29,30]:

$$H_2O_2+Fe^{2+}\rightarrow Fe^{3+}+OH^-+{}^{\bullet}OH \quad (5)$$

$$RH+{}^{\bullet}OH\rightarrow R^{\bullet}+H_2O \quad (6)$$

where,

RH is organic pollutant

$$R^{\bullet}+Fe^{3+}\rightarrow R^{+}+Fe^{2+} \quad (7)$$

$$Fe^{2+}+{}^{\bullet}OH\rightarrow Fe^{3+}+OH^- \quad (8)$$

In acidic medium, $^{\bullet}OH$ radicals are generated through H_2O_2 and Fe^{2+} as shown in Eq. (5). These $^{\bullet}OH$ radicals are responsible for the degradation of organic pollutants.

The present study deals with the treatment of BA from aqueous solution by acid precipitation followed by EC and EF processes separately. Both electrochemical studies were optimized using central composite design (CCD) in response surface methodology (RSM). RSM is an efficient and excellent tool for process optimization. It allows fewer number of experiments with rapid interpretation and is widely used for experimental design [31-34]. Here RSM in Design Expert Software (DES) was used for the effective optimization of different parameters such as pH, current density (CD), electrolyte concentration, H_2O_2 concentration and electrolysis time for the removal of BA and COD with minimal energy consumption (E.consumption).

MATERIALS AND METHODS

1. Chemicals

Analytical reagent grade chemicals were used in this study. Benzoic acid ($C_7H_6O_2$) and sodium sulfate (Na_2SO_4) were procured from Loba Chemie Pvt. Ltd., Mumbai (India). Sulfuric acid (H_2SO_4), sodium hydroxide (NaOH), potassium dichromate ($K_2Cr_2O_7$), acetic acid (CH_3COOH), mercury (II) sulfate ($HgSO_4$), methanol (CH_3OH), isopropyl alcohol (C_3H_8O), silver sulfate (Ag_2SO_4) and hydrogen peroxide (H_2O_2) (30% w/v) were supplied by Ranbaxy Fine Chemical Limited, New Delhi (India).

2. Synthetic BA Solution

Synthetic aqueous solution of benzoic acid was prepared by dissolving the requisite amount of BA in distilled water. To avoid microorganism's growth and unwanted biodegradation, all the reagents and samples were preserved at 4 °C. Working concentration of benzoic acid (400 mg/L) was chosen according to previous studies [35-37]. Initial COD of solution was determined as 751 mg/L.

3. Sample Analysis

Standard analytical methods were used for the measurement of COD, pH and ferrous ions concentration as given by the American Public Health Association (APHA) [38]. Concentration of BA and COD was analyzed by HPLC (Waters, USA) using UV detector with a wavelength of 240 nm [39-41] and COD analyzer (Aqualytic, Germany), respectively. Samples were filtered through nylon syringe filter (0.21 μm) before each analysis. The HPLC system was operated

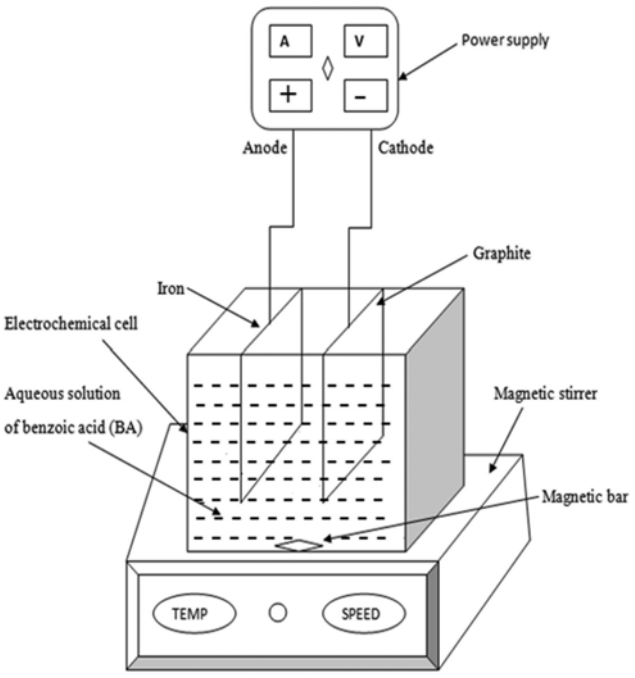

Fig. 1. Schematic diagram of experimental setup for electrochemical treatment.

Table 1. Operating parameters and their levels obtained from the statistical software for EC process

Levels	Central composite design characteristics			
	Parameter (range)			
	X_1 pH (3-11)	X_2 CD (A/m^2) (15.24→76.21)	X_3 Electrolyte concentration (mol/L) (0.03→0.07)	X_4 Time (min) (15→95)
$-2(-\alpha)$	3	15.24	0.03	15
−1	5	30.48	0.04	35
0	7	45.73	0.05	55
+1	9	60.97	0.06	75
$+2(\alpha)$	11	76.21	0.07	95

at ambient temperature with a mobile phase solution of 91% Millipore water, 7% isopropyl alcohol and 2% acetic acid of 1.2 mL/min flow rate in C18 column under isocratic mode [18,42]. Percentage removal of BA, COD and E.consumption (kWh/kg $COD_{removed}$) were calculated according to Eq. (9) and (10), respectively [43].

$$\% \text{ Removal of BA and COD} = \frac{C_i - C_f}{C_i} \times 100 \quad (9)$$

where, C_i & C_f are initial and final concentration of BA or COD

$$\text{E.consumption (kWh/kg}COD_{removed}) = \frac{VIT \times 100}{(\% \text{ Removal of COD}) C_{CODi} \times V_S} \times 100 \quad (10)$$

where V, I, T, C_{CODi} and V_S are voltage, current (amp), time (hour), initial COD (mg/L) and volume of solution (liter), respectively.

4. Experimental Procedure

4-1. Acid Precipitation

Acid was precipitated by adding 1 N H_2SO_4 to the solution having initial pH 4.6. Initial pH of the solution was adjusted to 3, 2, and 1 at different temperatures (15-60 °C). Settling was allowed for 4 hours for the precipitated solution; then, supernatant was filtered

Table 2. Operating parameters and their levels obtained from the statistical software for EF process

Levels	Central composite design characteristics			
	Parameter (range)			
	X_1 pH (1-5)	X_2 CD (A/m^2) (15.24→76.21)	X_3 H_2O_2 (mg/L) (100→500)	X_4 Time (min) (15→95)
$-2(-\alpha)$	1	15.24	100	15
−1	2	30.48	200	35
0	3	45.73	300	55
+1	4	60.97	400	75
$+2(\alpha)$	5	76.21	500	95

Table 3. Actual and CCD predicted removal efficiencies of BA, COD and E.consumption for EC process

Run no.	Independent variables				% Removal of BA: (R_1)		% Removal of COD: (R_2)		Energy consumption (kWh/kg $COD_{removed}$): (R_3)	
	X_1: (p^H)	X_2: (CD) (A/m^2)	X_3: (Na_2SO_4) (mole/L)	X_4: (t) (min)	Actual (exp.)	CCD predicted	Actual (exp.)	CCD predicted	Actual (exp.)	CCD predicted
1	5	30.48	0.04	75	43.85	45.99	42.99	45.51	28.19	26.16
2	9	30.48	0.04	35	42.96	50.33	36.39	43.85	15.54	15.78
3	5	60.97	0.06	35	52.37	57.57	50.29	50.98	33.74	32.85
4	9	60.97	0.07	75	54.09	52.42	54.19	52.35	67.10	66.97
5	5	30.48	0.06	35	43.27	45.22	37.89	41.22	14.92	11.24
6	9	30.48	0.06	75	59.46	63.39	52.29	58.48	23.18	21.62
7	5	60.97	0.06	75	73.09	71.89	64.09	63.74	56.73	60.44
8	9	60.97	0.06	35	51.31	53.42	52.29	53.21	32.45	32.85
9	7	45.72	0.05	55	72.09	76.60	69.39	65.83	22.70	24.96
10	7	45.72	0.06	55	70.46	72.81	68.79	64.11	23.21	26.38
11	5	30.48	0.04	35	36.09	31.94	37.29	34.08	15.16	15.78
12	11	30.48	0.04	75	38.31	36.40	35.39	34.28	30.01	33.63
13	5	60.97	0.04	75	64.29	67.58	60.29	63.35	60.31	55.90
14	9	60.97	0.06	15	38.96	36.14	40.39	39.25	18.00	19.06
15	5	30.48	0.06	95	55.45	54.93	54.39	52.72	28.22	26.82
16	9	15.24	0.06	35	43.20	39.88	39.09	34.64	05.42	08.42
17	5	60.97	0.06	55	55.99	57.57	48.19	50.98	35.21	32.85
18	9	60.97	0.06	75	53.96	60.65	55.89	59.71	65.06	60.44
19	7	45.72	0.04	55	71.31	70.37	67.09	63.87	24.84	26.38
20	7	45.72	0.05	75	73.36	77.36	72.09	68.75	30.67	34.46
21	3	45.72	0.05	55	40.09	38.95	46.69	45.66	35.69	34.92
22	9	45.72	0.05	55	66.36	69.87	62.09	64.44	26.84	27.45
23	7	30.48	0.05	55	62.64	66.32	56.59	58.00	15.70	14.79
24	7	60.97	0.05	55	76.64	76.37	67.09	68.56	39.74	40.46
25	7	45.72	0.04	35	64.74	62.87	61.09	56.66	17.36	16.89
26	7	76.21	0.05	55	71.09	65.64	63.09	60.17	61.64	61.29
27	7	45.72	0.05	35	68.44	66.72	59.99	59.78	17.67	15.47
28	7	30.48	0.05	75	63.34	67.40	57.29	59.43	21.15	19.98
29	7	30.48	0.05	35	54.34	56.12	47.29	49.44	11.96	09.60
30	7	60.97	0.04	55	68.09	74.77	63.39	67.12	35.05	39.60

Table 4. Actual and CCD predicted removal efficiencies of BA, COD and E.consumption for EF process

Run no.	Independent variables				% Removal of BA: (R_1)		% Removal of COD: (R_2)		Energy consumption (kWh/kg $COD_{removed}$): (R_3)	
	X_1: (p^H)	X_2: (CD) (A/m^2)	X_3: (H_2O_2) (mg/L)	X_4: (t) (min)	Actual (exp.)	CCD predicted	Actual (exp.)	CCD predicted	Actual (exp.)	CCD predicted
1	2	30.48	200	75	61.06	62.70	57.22	58.88	21.18	18.35
2	4	30.48	200	35	60.00	68.33	53.67	59.48	10.53	8.90
3	2	60.97	400	35	68.43	73.38	63.9	64.63	26.55	24.87
4	4	60.97	500	75	71.30	69.61	69.4	67.97	52.39	50.18
5	2	30.48	400	35	60.48	62.29	51.7	54.8	10.94	11.67
6	4	30.48	400	75	76.01	79.80	70.34	75.43	17.23	16.85
7	2	60.97	400	75	80.30	86.55	78.32	77.32	46.42	47.04
8	4	60.97	400	35	68.52	69.85	66.52	67.17	25.51	24.18
9	3	45.72	300	55	84.30	91.57	81.62	80.19	19.02	20.53
10	3	45.72	400	55	81.07	92.02	76.02	79.05	19.37	20.53
11	2	30.48	200	35	53.30	50.44	51.52	48.52	10.97	13.38
12	5	30.48	200	75	59.52	55.23	54.62	51.20	22.19	23.85
13	2	60.97	200	75	81.50	84.39	74.52	77.99	48.79	47.04
14	4	60.97	400	15	56.17	53.83	54.62	53.52	13.31	14.72
15	2	30.48	400	95	72.66	72.26	68.62	67.75	22.37	23.30
16	4	15.24	400	35	59.87	56.92	54.45	50.75	03.89	04.48
17	2	60.97	400	55	73.20	73.38	62.42	64.63	27.18	24.98
18	4	60.97	400	75	71.17	75.59	70.12	73.13	51.81	50.22
19	3	45.72	200	55	85.02	82.20	81.32	78.90	20.49	20.03
20	3	45.72	300	75	84.70	84.69	88.32	82.70	25.73	29.13
21	1	45.72	300	55	57.30	57.2	61.09	60.08	27.28	27.99
22	4	45.72	300	55	83.57	85.58	76.32	79.20	21.83	21.32
23	3	30.48	300	55	79.85	81.34	70.82	72.11	12.55	10.86
24	3	60.97	300	55	86.85	91.21	81.32	82.02	32.79	33.49
25	3	45.72	200	35	81.95	81.10	75.32	72.59	14.08	13.43
26	3	76.21	300	55	84.87	84.32	77.32	74.51	50.29	51.24
27	3	45.72	300	35	83.65	82.69	75.80	74.55	13.99	13.43
28	3	30.48	300	75	79.55	82.02	71.52	73.39	16.94	15.88
29	3	30.48	300	35	71.55	71.90	61.52	63.73	09.19	0.35
30	3	60.97	200	55	84.90	85.05	77.01	81.82	28.86	33.49

through Whatman filter paper (11-μm) and further treated by electrochemical processes.

4-2. Electrochemical Treatment

Both EC and EF experiments were performed in a plexiglass-made rectangular open batch cell containing 1 liter of solution and equipped with a graphite cathode (100 mm×80 mm×3 mm) and an iron anode (100 mm×80 mm×1 mm). Spacing between parallel electrodes was 2 cm and effective electrode area into solution was 131.2 cm^2. Fig. 1 shows a schematic diagram of the electrochemical experimental setup. Electrodes were cleaned and washed with H_2SO_4 solution (5% v/v) and distilled water between each successive run. Direct current (0-5 A) and voltage (0-25 V) was used to power parallel connected electrodes. Both treatments were performed at room temperature (25±2 °C) and atmospheric pressure. pH of aqueous solution was adjusted through 1 N H_2SO_4 and 1 N NaOH during experiments. Different concentrations of sodium sulfate were used as a supporting electrolyte for EC process and the only optimized value of electrolyte concentration (0.05 mol/L) was used in EF process. Desired amount of hydrogen peroxide (H_2O_2) was added to the reactor before the supply of electrical current in EF process. The range of operating parameters was determined by initial test runs for EC and EF processes as shown in Tables 1 and 2. Entire EC and EF experiments were performed at operating conditions predicted by RSM, and their corresponding CCD results are shown in Tables 3 and 4, respectively.

RESULTS AND DISCUSSION

1. Effect of Operating Parameters on Removal of BA, COD and E.consumption

1-1. Effect of Acid Precipitation on Removal of BA and COD

Benzoic acid (BA) is present in the ionized state in aqueous solution, as the pKa value for BA is 4.2. As pH (Initial pH- 4.6) of aqueous solution was decreased by adding H_2SO_4, the acid gets deionized

and concentration of hydrogen ions increases in the solution. Due to the common-ion (hydrogen ions) effect, ionic product value of BA surpasses its solubility product value, resulting in precipitation of BA [44]. Effect of pH on percentage removal of BA and COD at different temperatures was studied during acid precipitation process as shown in Fig. 2(a) and (b). Maximum removal of BA and COD was obtained as 61% and 56% at pH 1 and temperature 15 °C. The filtered supernatant (BA- 156 mg/L and COD-330 mg/L) was further treated by EC and EF processes separately at operating conditions obtained from RSM.

1-2. Effect of pH on Removal of BA, COD and E.consumption

pH is an important parameter in electrochemical treatment. To study the effect of initial pH, the aqueous solution was adjusted to desired pH in the range of 3-11 during EC and 1-5 during EF

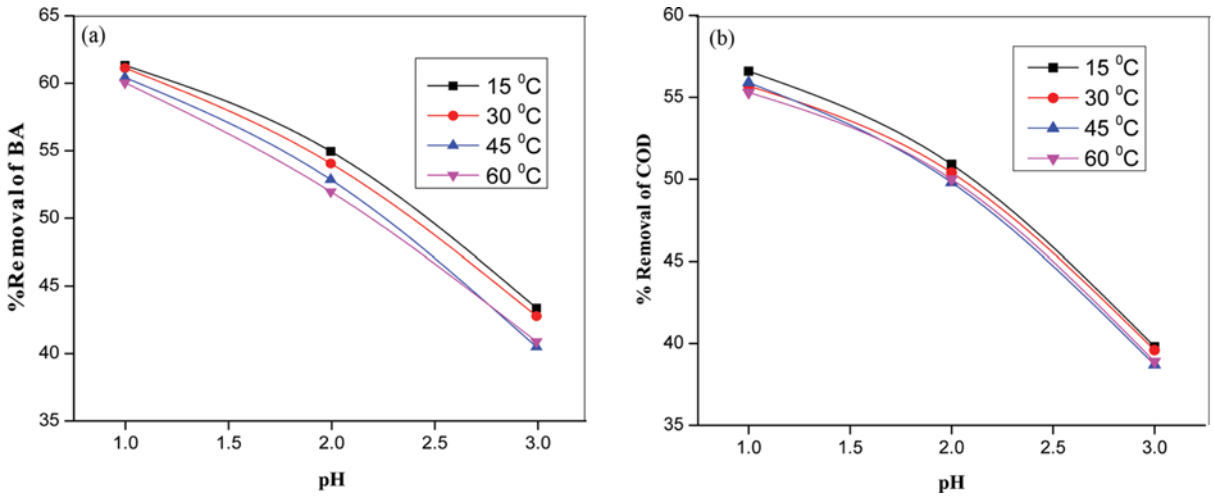

Fig. 2. Effect of pH at different temperatures in acid precipitation process (a) on removal of BA (b) on removal of COD.

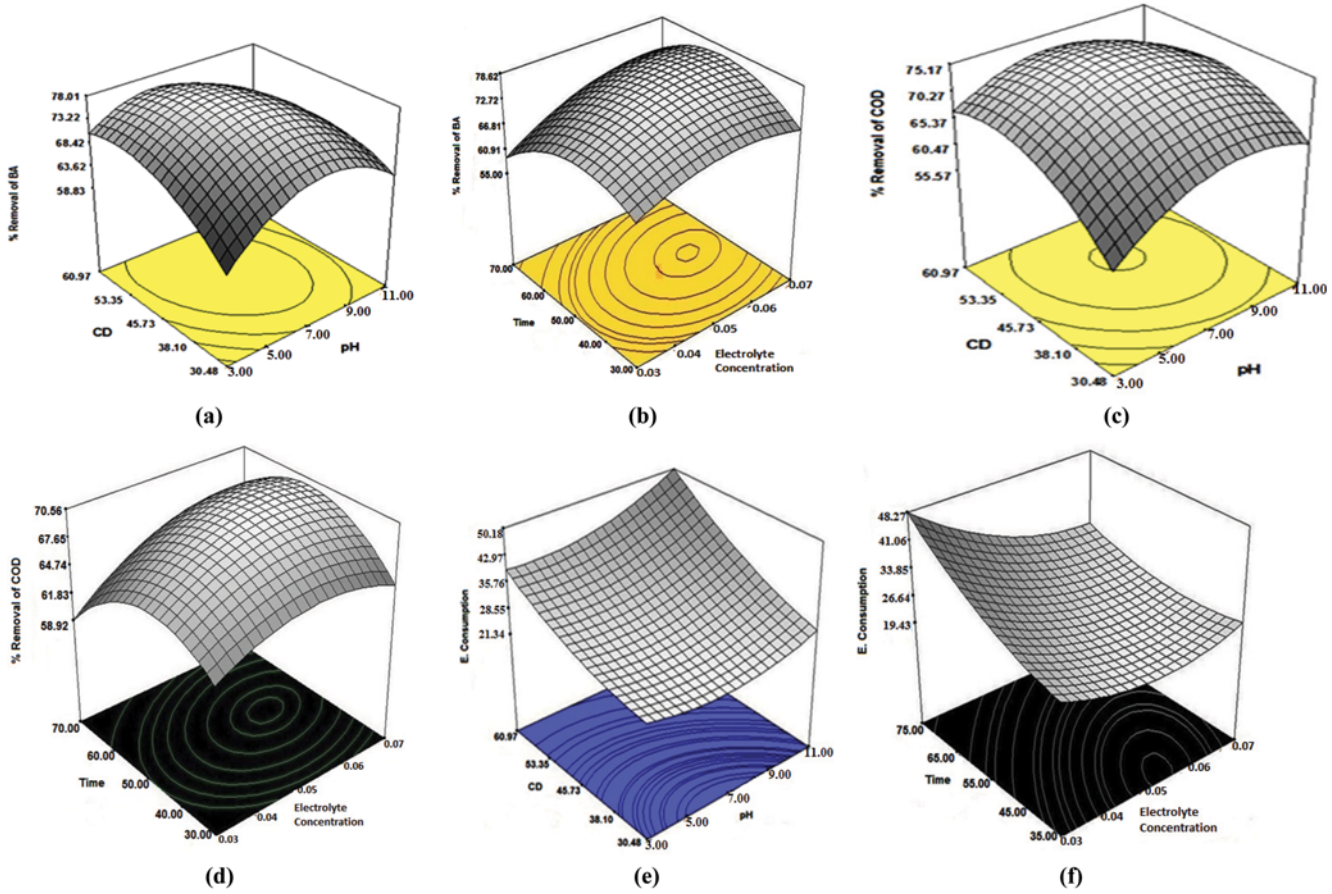

Fig. 3. Effect of pH, CD, time and electrolyte concentration on removal of BA, COD and E.consumption for EC.

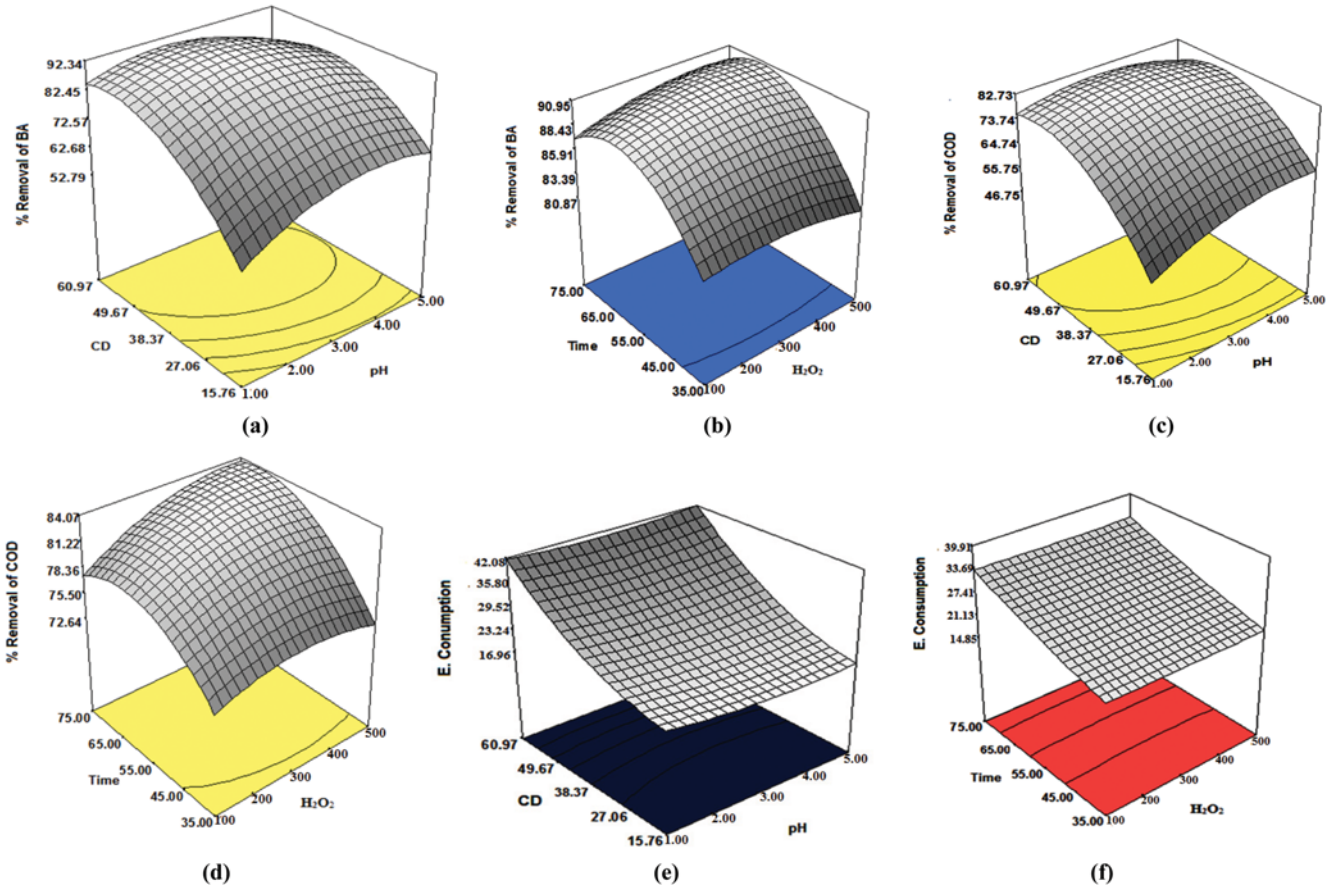

Fig. 4. Effect of pH, CD, time and H_2O_2 on removal of BA, COD and E.consumption for EF.

treatments. Effect of pH on % removal of BA and COD is shown in Figs. 3(a) and (c) and 4(a) and (c) for EC and EF processes, respectively. During electrolysis, Fe^{2+} ions are generated at the anode, which binds anionic colloidal particles and neutralizes their charges. Concentration of metal hydroxides increases with pH, which enhances the rate of adsorption of organic pollutants on amorphous metal hydroxide precipitates [45]. At very high pH (>9), removal efficiencies decreased due to weak interaction of metal hydroxide ions with suspension impurities [46]. In EF, removal of BA and COD was higher at acidic pH due to formation of metal hydroxide flocs as well as HO$^{\bullet}$ radicals, by addition of H_2O_2 as shown in Eq. (5) [47, 48]. At very low pH, oxonium ion ($H_3O_2^+$) is generated instead of HO$^{\bullet}$ radicals, and under basic condition H_2O_2 decomposes into water and oxygen resulting in lower removal [30,49]. Consumption of electrical energy varies with pH and reaches a minimum at pH-7.34 for EC and 2.99 for EF as shown in Figs. 3(e) and 4(e). Also, initial pH of the solution increased with time. The hydroxyl radicals produced in the reaction were not counter-balanced through the oxidation of water at anode. When the pH (corresponding to optimum conditions as predicted by CCD) of the solution was adjusted at 7.34 and 2.99 in EC and EF processes, respectively, an increase in pH of solution was observed as shown in Fig. 5. After 55 min, the pH of the solution increased from 7.34 and 2.99 to 8.82 and 3.90, during EC and EF processes, respectively. The solution pH further increased to 9.6 and 4.92 after 95 min of electrolysis

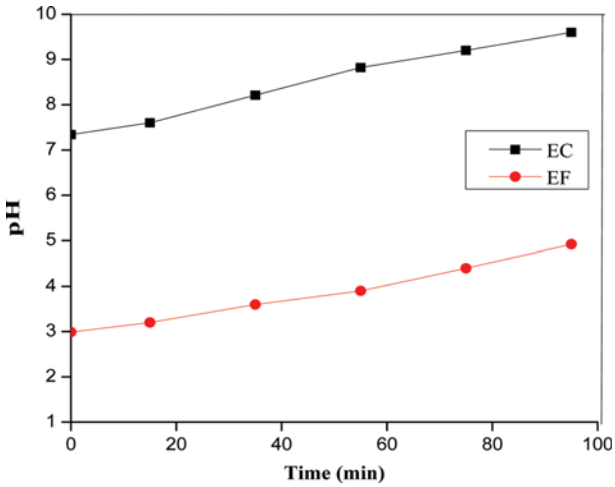

Fig. 5. Change in pH with time at optimum operating conditions in EC and EF processes.

during EC and EF processes, respectively. Removal efficiency was found less in unregulated pH system as compared to the regulated system. To achieve the higher removal efficiency, the pH was regulated during the experiments by adding 1 N H_2SO_4 at regular intervals. Nideesh et al. (2014) also observed that the removal efficiencies in the case of pH regulated system were higher as com-

pared to the unregulated system for the removal of Rhodamine B by peroxicoagulation process [50].

1-3. Effect of Current Density and Electrolysis Time on Removal of BA, COD and E.consumption

Current density and electrolysis time play vital roles in electrochemical processes. In this study a number of experiments involved using various current densities (15.24-76.21 A/m^2) and different slots of time (15-95 minutes) in both electrochemical processes. Higher current density favors greater amount of charge generation, which enhances removal. Furthermore, increasing current density also favors metal dissolution and generation of hydroxyl radicals (HO$^\bullet$). Effect of current densities on % removal of BA and COD is shown in Figs. 3(a) and (c) and 4(a) and (c) for EC and EF processes, respectively. Beyond optimum current density, i.e., 50.97 A/m^2 for EC and 44.87 A/m^2 for EF, removal efficiencies decreased owing to longer duration wherein Fe^{2+} ions and dissolved oxygen became rate-limiting factors. After some time, electrolysis consumes a considerable amount of charge in some side reactions and lastly corrosion of electrodes intensifies. Simultaneously, metal ion concentration and formation of HO$^\bullet$ radicals also increase with electrolysis time at a particular current density, pH and supporting electrolyte concentration. Beyond optimum time (58.86 min for EC and 55.10 min for EF), generation of metal ions and HO$^\bullet$ radicals is reduced, resulting in lower removal as shown in Figs. 3(b) and (d) and 4(b) and (d) for EC and EF processes, respectively. E.consumption is strongly dependent on current density and time as shown in Eq. (10). Beyond optimum values the percentage removal decreases; therefore, E.consumption increases. The results are shown in Figs. 3(e) and (f) and 4(e) and (f).

1-4. Effect of Electrolyte Concentration and H_2O_2 Dosages on the Removal of BA, COD and E.consumption

Supporting electrolyte is an important parameter in electrolysis for the improvement of solution conductivity and enhancement of electron transfer rate. We used different concentrations (0.03-0.07 mol/L) of sodium sulfate as a supporting electrolyte in the EC process. The optimum value was found to be 0.05 mol/L as shown in Figs. 3(b) and (d). This optimum concentration of sodium sulfate was also used in EF treatment. To get the maximum effectiveness of the EF process, the optimal concentration of H_2O_2 is highly important. Anodic iron diffuses the ions, which catalyzes the formation of HO$^\bullet$ radicals under acidic condition as shown in Eq. (5). Different concentrations of H_2O_2 (100-500 mg/L) were used during EF treatment and an optimal value (307 mg/L) was obtained as shown in Figs. 4(b) and (d). Beyond the optimum concentration of H_2O_2, the removal efficiencies decreased. This may be because excess amount of hydrogen peroxide shows scavenging effect on hydroxyl radicals [32,51] as shown below.

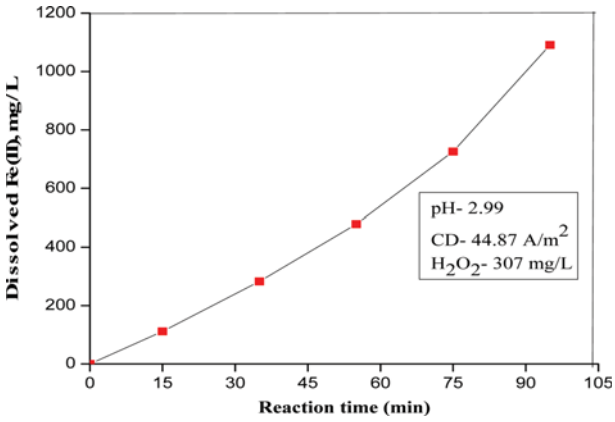

Fig. 6. Concentration of ferrous ions (Fe^{2+}) in solution with reaction time at optimum conditions.

$$H_2O_2+HO^\bullet \rightarrow HO_2^\bullet+H_2O \quad (11)$$

The above reaction leads to the formation of hydroperoxyl radicals which have much less oxidizing strength as compared to HO$^\bullet$ radicals [52]. Effects of electrolyte and H_2O_2 concentration on E.consumption are shown in Figs. 3(f) and 4(f), respectively.

1-5. Effect of Fe^{2+} Concentration

Concentration of ferrous ions plays an important role in the EF process [53]. Fe^{2+} ions in electrolytic solution enhance the concentration of the main oxidizing agent (HO$^\bullet$) [49]. Ferrous (Fe^{2+}) ions emerge from iron anode and are converted into ferric ions (Fe^{3+}) in the presence of H_2O_2. Coagulating nature of Fe^{3+} leads to the formation of sludge with Fe $(OH)_3$ [54]. However, an excess amount of Fe^{2+} ions in electrolyte solution causes consumption of hydroxyl radicals and affects the extent of removal [55]. Concentrations of dissolved ferrous ions with time at optimum operating conditions during EF treatment are shown in Fig. 6.

2. Response Surface Methodology Study

2-1. Optimization

The entire electrochemical processes were optimized for maximal removal of BA, COD with minimal E.consumption based on CCD values. All operating conditions and their corresponding experimental run values for EC and EF processes are given in Tables 3 and 4, respectively. The optimum conditions were reconfirmed by performing test runs and the optimized result obtained was as shown in Table 5. Closeness of CCD predicted values and test run values indicates good adequacy of the model.

2-2. Regression Model Equations Based on ANOVA Analysis for EC and EF Processes

We used second-order regression model equations for correla-

Table 5. Optimum operating conditions predicted by CCD and experimental test run by EC and EF processes

	pH	CD (A/m^2)	Electrolyte conc^n (mole/L)	H_2O_2 conc^n (mg/L)	Time (min)	% Removal of BA		% Removal of COD		Energy consumption (kWh/kg $COD_{removed}$)	
						CCD (pre.)	Test run	CCD (pre.)	Test run	CCD (pre.)	Test run
EC	7.34	50.97	0.05	-	58.86	76.83	71.60	69.23	64.87	30.86	33.06
EF	2.99	44.87	-	307	55.10	88.50	85.86	82.21	74.78	21.15	25.17

tions between responses and independent variables. Responses (R_1, R_2 and R_3) for both electrochemical processes are given below:

Generalized equation:

Second-order regression model equations were used for correlations between responses and independent variables. Responses (R_1, R_2 and R_3) for both electrochemical processes are given below:

Generalized equation:

$$R_i=b_0+b_1\times pH+b_2\times j+b_3\times C_i+b_4\times t+b_{11}\times pH^2+b_{22}\times j^2+b_{33}\times C_i^2 +b_{44}\times t^2+b_{12}\times pH\times j+b_{13}\times pH\times C_i+b_{14}\times pH\times t+b_{23}\times j\times C_i+b_{24} \times j\times t+b_{34}\times C_i\times t \quad (12)$$

where

j- Current density, C_1- Sodium Sulfate concentration, C_2- H_2O_2 concentration, t-Time

BA

$$R_1^{EC}=76.60+1.79\times pH+5.03\times j+2.22\times C_1+5.32\times t-8.52\times pH^2 -5.25\times j^2-2.01\times C_1^2-4.56\times t^2-3.46\times pH\times j-2.18\times pH\times C_1 -1.77\times pH\times t-2.63\times j\times C_1-0.32\times j\times t+0.38\times C_1\times t \quad (13)$$

$$R_1^{EF}=91.55+0.022\times pH+4.22\times j+1.09\times C_2+4.30\times t-7.52\times pH^2 -4.96\times j^2+0.34\times C_2^2-6.11\times t^2\ 4.17\times pH\times j-1.60\times pH\times C_2 -3\times pH\times t-2.66\times j\times C_2-1.86\times j\times t-0.55\times C_2\times t \quad (14)$$

COD

$$R_2^{EC}=67.84+1.43\times pH+5.28\times j+1.62\times C_1+4.48\times t-4.83\times pH^2 -4.56\times j^2-2.34\times C_1^2-3.57\times t^2-1.62\times pH\times j-0.26\times pH\times C_1 -1.57\times pH\times t-2.53\times j\times C_1-0.51\times j\times t+0.84\times C_1\times t \quad (15)$$

$$R_2^{EF}=81.62+1.36\times pH+4.60\times j-0.033\times C_2+4.97\times t-5.97\times pH^2 -4.90\times j^2-0.24\times C_2^2-3.99\times t^2-2.68\times pH\times j-0.54\times pH\times C_2 -2.94\times pH\times t-2.81\times j\times C_2-0.64\times j\times t-0.075\times C_2\times t \quad (16)$$

E.consumption

$$R_3^{EC}=24.37-0.91\times pH+12.86\times j+0.047\times C_1+9.64\times t+2.46\times pH^2 +2.80\times j^2+0.65\times C_1^2+1.23\times t^2+0.42\times\ pH\times j+0.79\times pH\times C_1 +1.17\times pH\times t+2.28\times j\times C_1+4.70\times j\times t-0.16\times C_1\times t \quad (17)$$

$$R_3^{EF}=20.3-0.22\times pH+11.3\times j-0.32\times C_2+7.85\times t+1.64\times pH^2 +2\times j^2+0.18\times C_2^2+1.25\times t^2+0.91\times pH\times j-0.11\times pH\times C_2 +1.21\times pH\times t+0.58j\times C_2+4.08\times j\times t-0.071\times C_2\times t \quad (18)$$

3. Sludge Analyses

Sludge generated after EC and EF treatments at optimum operating conditions was analyzed by the following techniques.

3-1. Settling, Point of Zero Charge (PZC) and FTIR

3-1-1. Settling

The settling experiments of sludge obtained by EC and EF methods were done according to a given standard method [38] in a glass cylinder having capacity of 1 liter. Position of sludge supernatant interface with time is shown in Fig. 7(a). At time t=0, thte level of EC generated sludge was (9 cm) more than EF generated sludge (7.3 cm). The level of EC generated sludge after 1 min was 8.5 cm, which was

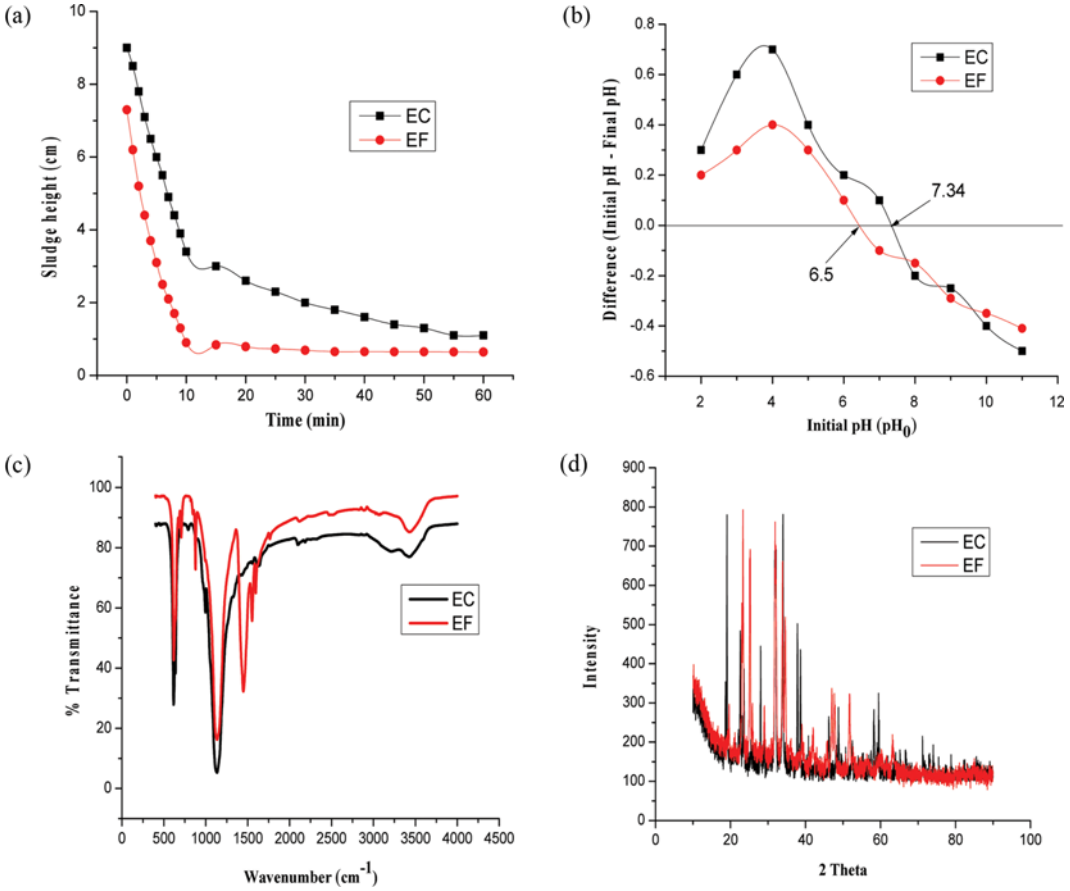

Fig. 7. (a) Settling characteristics (b) point of zero charge (c) FTIR spectra (d) XRD spectra (e) & (f) SEM images (g) & (h) DTA/TGA graphs obtained of EC and EF generated sludge.

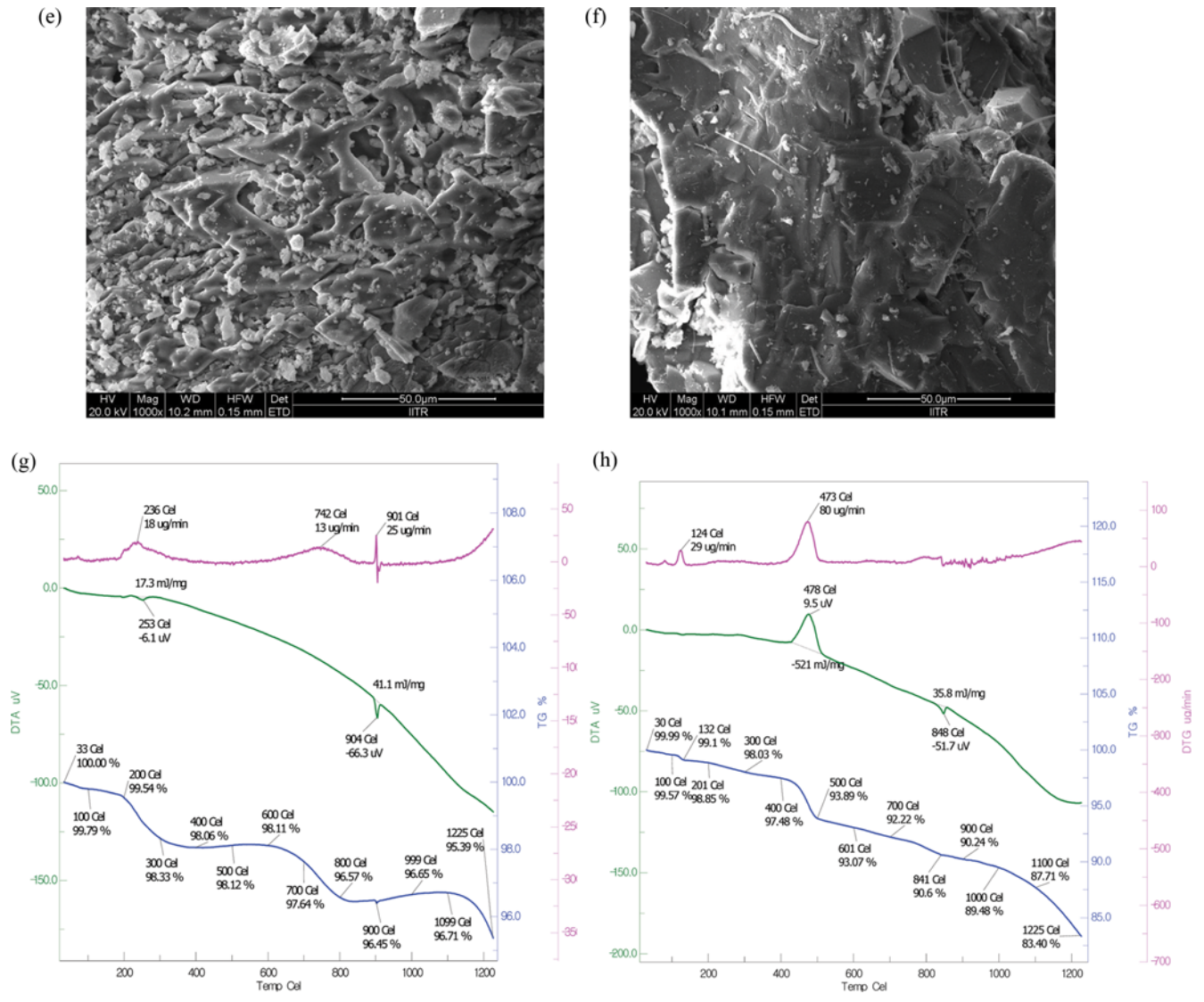

Fig. 7. Continued.

more than the sludge generated by EF process (6.2 cm). The settling level of EC and EF generated sludge was found constant at 1.1 cm and 0.65 cm after 50 and 35 min, respectively. Results indicate high settling characteristics of EF generated sludge as compared to EC generated sludge.

3-1-2. PZC

PZC is a function of pH where a solid submerged in the electrolyte displays a zero net charge at the surface of solid material. In the present study, salt addition method as contained in American Society for Testing of Materials (ASTM) D-3838-05 was used for the determination of PZC [56]. The intersection point on the resulting curve plotted between ΔpH [$\Delta pH=pH_0$ (Initial pH)−pH_f (Final pH)] and initial pH (pH_0) at ΔpH=0 provides PZC. Anion adsorption is favored at pH<PZC, i.e., surface positively charged while cation adsorption is favored at pH>PZC, i.e., surface negatively charged. PZC values for EC and EF generated sludge are 7.34 and 6.5, respectively, as shown in Fig. 7(b).

3-1-3. FTIR

FTIR spectra of generated sludge by EC and EF processes are shown in Fig. 7(c). Presence of various functional groups in the sludge samples indicates electrolyte interaction between cations and flocs, which are responsible for removal of colloids during treatment. In the FTIR spectra the broad and intense bands 3,325.69 cm^{-1}, 3,432.15 cm^{-1} are attributed to stretching vibrations of hydroxyl group and characteristics of hydrogen ring. Wavelengths 1,614.24 cm^{-1}, 1,550 cm^{-1}, 1,446.48 cm^{-1} and 1,147 cm^{-1} show the presence of C=C, C=O, C-H and C-O-C, respectively. Peaks are observed in the range of 600 cm^{-1} to 500 cm^{-1} depicted the C-X stretching.

3-2. XRD, SEM/EDX, DTA/TGA

3-2-1. XRD

XRD spectra of sludge obtained by EC and EF methods are shown in Fig. 7(d). Basically, the XRD spectrum tells about the morphology and extent of crystallinity. XRD spectra of both EC and EF generated sludge indicate exceptionally shallow and broad diffraction peaks. Broad and lower intensity peaks of Bragg reflection show poor crystalline phase or more likely amorphous phase [44]. In this

Table 6. Elemental composition of sludge based on EDAX results for EC and EF processes

Element		C K	O K	Na K	S K	Fe K
Weight%	EC (sludge)	16.77	19.34	27.42	11.2	25.27
	EF (sludge)	12.58	25.52	23.64	17.53	20.73

study, EC generated sludge was found poorly crystalline in comparison to EF generated sludge at optimum operating condition.

3-2-2. SEM/EDX

SEM analysis gives an idea about surface structure: whether it is crystalline or amorphous. Sludge obtained after EC and EF treatment at optimum operating conditions was dried at 105 °C. It is inferred that EF-generated sludge has more porous structure compared to EC-generated sludge, as shown in Fig. 7(e) and (f). Thus, the particle size of EF-generated sludge stays more downcast than EC-generated sludge. Composition of elements (in weight percent) for EF- and EC-generated sludge through EDX analysis is given in Table 6. It was found that the weight percent of Fe and C was higher and weight percent of oxygen was lower in case of EC-generated sludge.

3-2-3. DTA/TGA

DTA/TGA analyses of EC and EF generated sludge are shown in Fig. 6(g) and (h). The analysis was performed in air atmosphere (flow rate 200 ml/min) and heated from ambient temperature to 1,200 °C with a heating rate of 10 K/min. TGA graphs for both the processes show three different oxidation stages. Oxidation rates of EC-generated sludge are higher in comparison to EF-generated sludge in each stage as shown in Fig. 7(g) and (h). Below 100 °C, EF and EC processes obtained sludge lost their weights by 0.43% and 0.21%, respectively. This is due to incomplete evaporation of pore solution at ambient temperature [57]. The rate of weight loss for EF- and EC-produced sludge was 0.08 mg/min to 0.018 mg/min. Reaction demonstrates an endothermic nature because of disintegration with early oxidation of various fragments of functional groups which are expelled during treatment and exothermic nature due to carbon chain discontinuity.

4. Operating Cost

In the present study total operating cost of EC and EF treatments was determined based on E.consumption, electrode consumption and chemical consumption (H_2O_2 in EF) at optimum conditions by Eq. (19) and presented in Table 7.

$$\text{Operating cost} = \text{Energy consumption (kWh/kgCOD}_{removed}\text{)} \times \text{ENC} + \text{Electrode consumption (kg/kgCOD}_{removed}\text{)} \times \text{ELC} + \text{Chemical consumption (kg/kgCOD}_{removed}\text{)} \times \text{CC} \quad (19)$$

where, ENC- Energy cost (Rs. 5.75/kWh), ELC- Electrode cost (Rs. 55/kg for Fe electrode) CC- Chemical cost (Rs.22/kg for H_2O_2 (30% w/v)). It may be concluded that the operating cost is lower for EF treatment. This is because the operating cost during EC treatment increases considerably due to high consumption of electricity and electrode material.

CONCLUSIONS

We investigated the removal of BA and COD from aqueous solution by acid precipitation followed by EC and EF methods. Approximately 61% of BA and 56% COD were removed from aqueous solution through acid precipitation pre-treatment step at pH 1 and temperature 15 °C. Maximum percentage removal of BA, COD and E.consumption (kWh/kgCOD$_{removed}$) were obtained 76.83, 69.23 and 30.86 at pH-7.34, CD- 50.97 A/m^2, time- 58.86 min, electrolyte concentration- 0.05 mol/L and 88.50, 82.21 and 21.15 at pH-2.99, CD- 44.87 A/m^2, time- 55.10 min, H_2O_2 concentration- 307 mg/L by EC and EF processes respectively. High correlation between models predicted values and actual responses was shown in this study. Therefore, based on removal efficiencies, energy consumption and operating cost of the EF process are more efficient than for the EC process.

ACKNOWLEDGEMENTS

Authors are thankful to the Department of Chemical Engineering, Indian Institute of Technology Roorkee, for providing technical facilities and Ministry of Human Resource Development, New Delhi, India for financial support.

SUPPORTING INFORMATION

Additional information as noted in the text. This information is available via the Internet at http://www.springer.com/chemistry/journal/11814.

REFERENCES

1. H. A. Wittcoff, B. G. Reuben and J. S. Plotkin, Industrial Organic Chemicals, 2nd Ed., Wiley-Interscience (2004).
2. R. Kleerebezem, L. W. Hulshoff Pol and G. Lettinga, *Biotechnol. Bioeng.*, **91**, 169 (2005).
3. G. R. Pophali, R. Khan, R. S. Dhodapkar, T. Nandy and S. Devotta, *J. Environ. Manage.*, **85**, 1024 (2007).
4. M. Karthik, N. Dafale, P. Pathe and T. Nandy, *J. Hazard. Mater.*,

Table 7. Operating cost during EC and EF process at optimum operating conditions given by CCD and experimental test runs

Treatment method		Energy consumed (kWh/kgCOD$_{removed}$)	Electrode consumed (kg/kg COD$_{removed}$)	Chemical consumed (H_2O_2) (kg/kg COD$_{removed}$)	Operating cost ($) 1 $=66 Rs.
EC	CCD based	30.86	2.60	-	4.86
	Test run based	33.06	2.80	-	5.21
EF	CCD based	21.15	1.50	1.13	4.63
	Test run based	25.17	1.57	1.23	5.18

154(1), 721 (2008).
5. J. P. Guyot, H. Macarie and A. Noyola, *Appl. Biochem. Biotechnol.*, **24/25**, 579 (1990).
6. H. Macarie and J. P. Guyot, *Appl. Microbiol. Biotechnol.*, **38**, 398 (1992).
7. J. C. Young, I. S. Kim, I. C. Page, D. R. Wilson, G. J. Brown and A. A. Cocci, *Water Sci. Technol.*, **42**, 277 (2000).
8. A. Noyola, W. Macarie and J. P. Guyot, *Environ. Technol.*, **11**, 239 (1990).
9. X. X. Zhang, S. P. Cheng, Y. Q. Wan, S. L. Sun, C. J. Zhu, D. Y. Zhao and W. Y. Pan, *Inter. Biodeter. Biodegr.*, **58**, 94 (2006).
10. M. Shirota, T. Seki, K. Tago, H. Katoh, H. Marumo, M. Furuya, T. Shindo and H. Ono, *J. Toxicol. Sci.*, **33**, 431 (2008).
11. US EPA, Part 136 (1992).
12. B. J. Thamer and A. F. Voigt, *J. Phys. Chem.*, **56**, 225 (1952).
13. X. X. Zhang, S. Sun, Y. Zhang, B. Wu, Z. Y. Zhang, B. Liu, L. Y. Yang and S. P. Cheng, *J. Hazard. Mater.*, **176**(1), 300 (2010).
14. R. B. Meyer, A. Fischbein, K. Rosenman, Y. Lerman, D. E. Drayer and M. M. Reidenberg, *Am. J. Med.*, **76**, 989 (1984).
15. L. Cui. Y. Shi, G. Dai, H. Pan, J. Chen, L. Song, S. Wang, H. C. Chang, H. Sheng and X. Wang, *Toxicol. Appl. Pharmcol.*, **210**, 24 (2006).
16. L. Cui, G. Dai, L. Xu, S. Wang, L. Song, R. Zhao, H. Xiao, J. Zhou and X. Wang, *Toxicology*, **201**, 59 (2004).
17. A. Wibbertmann, J. G. Kielhorn, I. Koennecker, C. Mangelsdorf and C. Melber, World Health Organization (2000).
18. S. Verma, B. Prasad and I. M. Mishra, *J. Hazard. Mater.*, **178**, 1055 (2010).
19. C. H. Wu, *React. Kinet. Catal. Lett.*, **90**, 301 (2007).
20. Central Pollution Control Board (CPCB) (2005).
21. A. Asghar, A. A. A. Raman and W. M. A. W Daud, *J. Cleaner Prod.*, **87**, 826 (2015).
22. M. A. Chon, A. K. Sharma, S. Burn and C. P. Saint, *J. Cleaner Prod.*, **35**, 230 (2012).
23. V. López-Grimau, M. C. Gutiérrez, J. Valldeperas and M. Crespi, *Color Technol.*, **128**, 36 (2011).
24. G. Chen, *Sep. Purif. Technol.*, **38**, 11 (2004).
25. P. K. Holt, G. W. Barton and C. A. Mitchell, *Chemosphere*, **59**, 355 (2005).
26. E. Brillas, I. Sires and M. A. Oturan, *Chem. Rev.*, **109**, 6570 (2009).
27. J. Li, Z. Ai and L. Zhang, *J. Hazard. Mater.*, **164**, 18 (2009).
28. E. Atmaca, *J. Hazard. Mater.*, **163**, 109 (2009).
29. E. Neyens and J. Baeyens, *J. Hazard. Mater.*, **98**, 33 (2003).
30. J. Ma, W. Song, C. Chen, W. Ma, J. Zhao and Y. Tang, *Environ. Sci. Technol.*, **395**, 5810 (2005).
31. S. Mohajeri, H. A. Aziz, M. H. Isa, M. A. Zahed and M. N. Adlan, *J. Hazard. Mater.*, **176**, 749 (2009).
32. M. Azama, M. Bahram, S. Nouri and A. Naseri, *J. Serb. Chem. Soc.*, **77**, 235 (2012).
33. S. Garcia-Seguraa, L. C. Almeidab, N. Bocchi and E. Brillas, *J. Hazard. Mater.*, **194**, 109 (2011).
34. J. Virkutyte, E. Rokhina and V. Jegatheesan, *Bioresour. Technol.*, **101**, 1440 (2010).
35. S. K. F. Marashi, H. R. Kariminia and I. S. P. Savizi, *Biotechnol. Lett.*, **35**(2), 197 (2013).
36. S. Verma, B. Prasad and I. M. Mishra, *Ind. Eng. Chem. Res.*, **50**(9), 5352 (2011).
37. K. K. Garg and B. Prasad, *J. Taiwan Inst. Chem. Eng.*, **56**, 122 (2015).
38. APHA, Washington DC, U.S.A. (1995).
39. K. K. Garg, B. Prasad and V. C. Srivastava, *Sep. Purif. Technol.*, **128**, 80 (2014).
40. K. K. Garg and B. Prasad, *J. Environ. Chem. Eng.*, **4**, 178 (2016).
41. R. Thiruvenkatachari, T. O. Kwon and I. S. Moon, *J. Environ. Sci. Health A Tox. Hazard. Subst. Environ. Eng.*, **41**, 1685 (2006).
42. T. Park, J. S. Lim, Y. Lee and S. Kim, *J. Supercrit. Fluids*, **26**, 201 (2003).
43. K. K. Garg and B. Prasad, *J. Environ. Chem. Eng.*, **3**, 1731 (2015).
44. S. Verma, B. Prasad and I. M. Mishra, *J. Hazard. Toxic Radioact. Waste.*, **18**(3), 04014013 (2014)
45. O. T. Can, M. Bayramoglu and M. Kobya, *Ind. Eng. Chem. Res.*, **42**, 3391 (2003).
46. J. P. Kushwaha, V. C. Srivastava and I. D. Mall, *Environ. Energy Eng.*, **57**, 2589 (2010).
47. M. Kallel, C. Belaid, R. Boussahel, M. Ksibi, A. Montiel and B. Elleuch, *J. Hazard. Mater.*, **163**, 550 (2009).
48. R. J. Watts, M. K. Foget, S. H. Kong and A. L. Teel, *J. Hazard. Mater.*, **69**, 229 (1999).
49. P. V. Nidheesh, R. Gandhimathi, *Desalination*, **299**, 1 (2012).
50. P. V. Nidheesh and R. Gandhimathi, *Environ. Sci. Pollut. Res.*, **21**, 8585 (2014).
51. H. Lee and M. Shoda, *J. Hazard. Mater.*, **153**, 1314 (2008).
52. M. I. Badawy and M. E. M. Ali, *J. Hazard. Mater.*, **136**, 961 (2006).
53. M. A. Oturan, N. Oturan, C. Lahitte and S. Trevin, *Electroanal. Chem.*, **507**, 96 (2001).
54. U. Kurt, O. Apaydin and M. T. Gonullu, *J. Hazard. Mater.*, **143**, 33 (2007).
55. T. S. N. S. Narayanan, G. Magesh and N. Rajendran, *Fresenius Environ. Bull.*, **12**, 776 (2003).
56. G. Song, C. Cao and S. H. Chen, *Corros Sci.*, **47**, 323 (2005).
57. ASTM, D 3838-05, Philadelphia PA, United State of America (2011).
58. K. K. Garg and B. Prasad, *J. Taiwan Inst. Chem. Eng.*, **60**, 383 (2016).